# Large full-thickness wounded skin regeneration using 3D-printed elastic scaffold with minimal functional unit of skin

**Peng Chang[1]** 🆔 , **Shijie Li[2], Qian Sun[3], Kai Guo[2], Heran Wang[2], Song Li[2], Liming Zhang[2], Yongbao Xie[2], Xiongfei Zheng[2] and Yunhui Liu[1,4]**

## Abstract
Traditional tissue engineering skin are composed of living cells and natural or synthetic scaffold. Besize the time delay and the risk of contamination involved with cell culture, the lack of autologous cell source and the persistence of allogeneic cells in heterologous grafts have limited its application. This study shows a novel tissue engineering functional skin by carrying minimal functional unit of skin (MFUS) in 3D-printed polylactide-co-caprolactone (PLCL) scaffold and collagen gel (PLCL + Col + MFUS). MFUS is full-layer micro skin harvested from rat autologous tail skin. 3D-printed PLCL elastic scaffold has the similar mechanical properties with rat skin which provides a suitable environment for MFUS growing and enhances the skin wound healing. Four large full-thickness skin defects with 30 mm diameter of each wound are created in rat dorsal skin, and treated either with tissue engineering functional skin (PLCL + Col + MFUS), or with 3D-printed PLCL scaffold and collagen gel (PLCL + Col), or with micro skin islands only (Micro skin), or without treatment (Normal healing). The wound treated with PLCL + Col + MFUS heales much faster than the other three groups as evidenced by the fibroblasts migration from fascia to the gap between the MFUS dermis layer, and functional skin with hair follicles and sebaceous gland has been regenerated. The PLCL + Col treated wound heals faster than normal healing wound, but no skin appendages formed in PLCL + Col-treated wound. The wound treated with micro skin islands heals slower than the wounds treated either with tissue engineering skin (PLCL + Col + MFUS) or with PLCL + Col gel. Our results provide a new strategy to use autologous MFUS instead "seed cells" as the bio-resource of engineering skin for large full-thickness skin wound healing.

[1]Department of Neurosurgery and Plastic and Reconstructive Surgery, Shengjing Hospital of China Medical University, Shenyang, China
[2]State Key Laboratory of Robotics, Shenyang Institute of Automation, Chinese Academy of Sciences, Shenyang, China
[3]Experimental Animal Center, General Hospital of Northern Center Command, Shenyang, China
[4]Liaoning Medical Surgery and Rehabilitation Robot Engineering Research Center, Shenyang, China

**Corresponding authors:**
Yunhui Liu, Department of Neurosurgery, Shengjing Hospital of China Medical University, 36 Sanhao Street, Shenyang 110004, China.
Email: liuyh@sj-hospital.org

Xiongfei Zheng, State Key Laboratory of Robotics, Shenyang Institute of Automation, Chinese Academy of Sciences, 114 Nanta steet, Shenyang 110000, China.
Email: zhengxiongfei@sia.cn

## Highlights

- A novel engineering skin with 3D-printed elastomer PLCL scaffold.
- MFUS replace traditional seed cells for functional skin regeneration by 3D bio-printing.
- A new strategy of tissue engineered skin for wound healing.

## Introduction

Skin is the largest organ covering the whole human body surface. Skin acts as an interface between the internal organs and the external environment forming a barrier to prevent the body dehydration and the penetration of external microorganisms.[1] The human skin comprises of three layers: epidermis (outermost), dermis (middle), and hypodermis (deeper).[2] Skin injuries are very common, and human skin has a natural ability to promote the self-regeneration for small skin defect. However, this capacity can be compromised under specific conditions, like extensive skin loss, deep burns, chronic wounds, non-healing ulcers, and diabetes.[3–5] Extreme loss of skin function and structure due to injury and illness will result in substantial physiological imbalance and may ultimately lead to major disability or even death.[6] Thus, the healing of large or chronic full-thickness wounds with functional skin regeneration is still a challenge in clinics so far.[7]

The use of skin grafts has shown the effective results on enhancing the skin wound healing. However, the limited donor-site skin yields another potential problem. Allografts and xenografts provide temporary coverage, but they can't stay a long time in the body due to the immunoreactions.[8,9] In addition, there might not be readily available skin allografts for use,[10] and the allografts carry some risks of infection and antigen exposure.[11]

Recent years, tissue engineering skin comprised mostly of human cell lines with degradable materials have been used for transplantation onto burned and wounded skin patients.[12] However, the time required to isolate and culture the cells is 2–3 weeks before they are suitable for grafting,[13] and such long culture time increases the risk of contamination. Furthermore, the seeded cells can not differentiate into all types of the cells needed for full-thickness skin reconstitution and they cannot form the functional skin structure because of the complexity of its organization.[14]

Autologous micro-skin grafting has been used for large skin wound healing due to it has smaller trauma to the donor area and larger amplification areas than traditional skin grafting method.[15] So far, micro skin islands used for covering wound only contain epidermal and part dermis, they can't regenerate full-thickness functional skin and the healed tissue has disorganized structure.[12] Although some researchers have shown better healing results by using full-layer micro skin, the operation of full-layer micro skin harvesting and implanting is time-consuming and healing by micro-skin only is slow.[13,15,16] Moreover, the micro-skin islands are difficultly attached to the wound area. Once the wound is infected, the tiny skin islands are easily necrosed by infection. Therefore, a scaffold used as a wound closure and micro-skin island carrier after large full-thickness skin defect is required to create a sealed wound environment to keep out infection, and also create a moist environment to promote the wound healing process and enhance the micro-skin island growth.[17]

Biomaterial scaffolds are increasingly being used to drive tissue regeneration.[18] Some biodegradable and biocompatible polymers have been used to protect open wounds, promote the cell growth, and suppress granulation tissue and scar.[19] These polymer scaffolds can be processed with adequate control of the architectural parameters such as pore size and shape, wall morphology, and surface area which are key issues for cell seeding, migration, growth, mass transport, and tissue formation. Among the different synthetic polymers, poly-ε-hydroxy esters such as polylactic acid (PLA), polyglycolide (PGA), and polycaprolactone (PCL) are the most used for regenerative medicine.[20,21] However, the synthetic polymer only is unable to restore skin function due to the lack of hydrophilicity for cell adhesion, as well as its limited biocompatibility.

Collagen, the major protein in skin plays a dominant role in maintaining the biological and structural integrity of the extracellular matrix (ECM), and is a dynamic and flexible material that undergoes constant remodeling to refine cellular behavior and tissue function.[22] It has been reported that the collagen-containing matrix can be used as an effective therapeutic agent for impaired diabetic wound healing.[23] The combination of collagen-containing polymer scaffold with cells has helped to reduce mortality in large burn, but the healed skin lack hair follicles and glands after transplantation.[13,24]

In this study, we propose a new concept for the first time to use the minimum functional unit of skin (MFUS) to instead of "seed cells" to develop a novel tissue engineering skin. Each MFUS is an autologous full-thickness cylindrical micro skin island which has complete skin structure including 1–3 hair follicles, some sweat glands, and other skin accessory organs. To harvest enough the MFUS in a short time, we invented an electronic punch which can punch and collect the MFUS simultaneously. To reduce the operation time and improve the survival rate of the MFUS, we developed a Three-dimensional (3D)-printed PLCL scaffold which has been designed with suitable pore size and structure used as a MFUS supporting sheet. It's well known that 3D-bioprinting can be customized for skin shape with cells and other materials distributed precisely, achieving rapid and reliable production of bionic skin substitutes, therefore, meeting
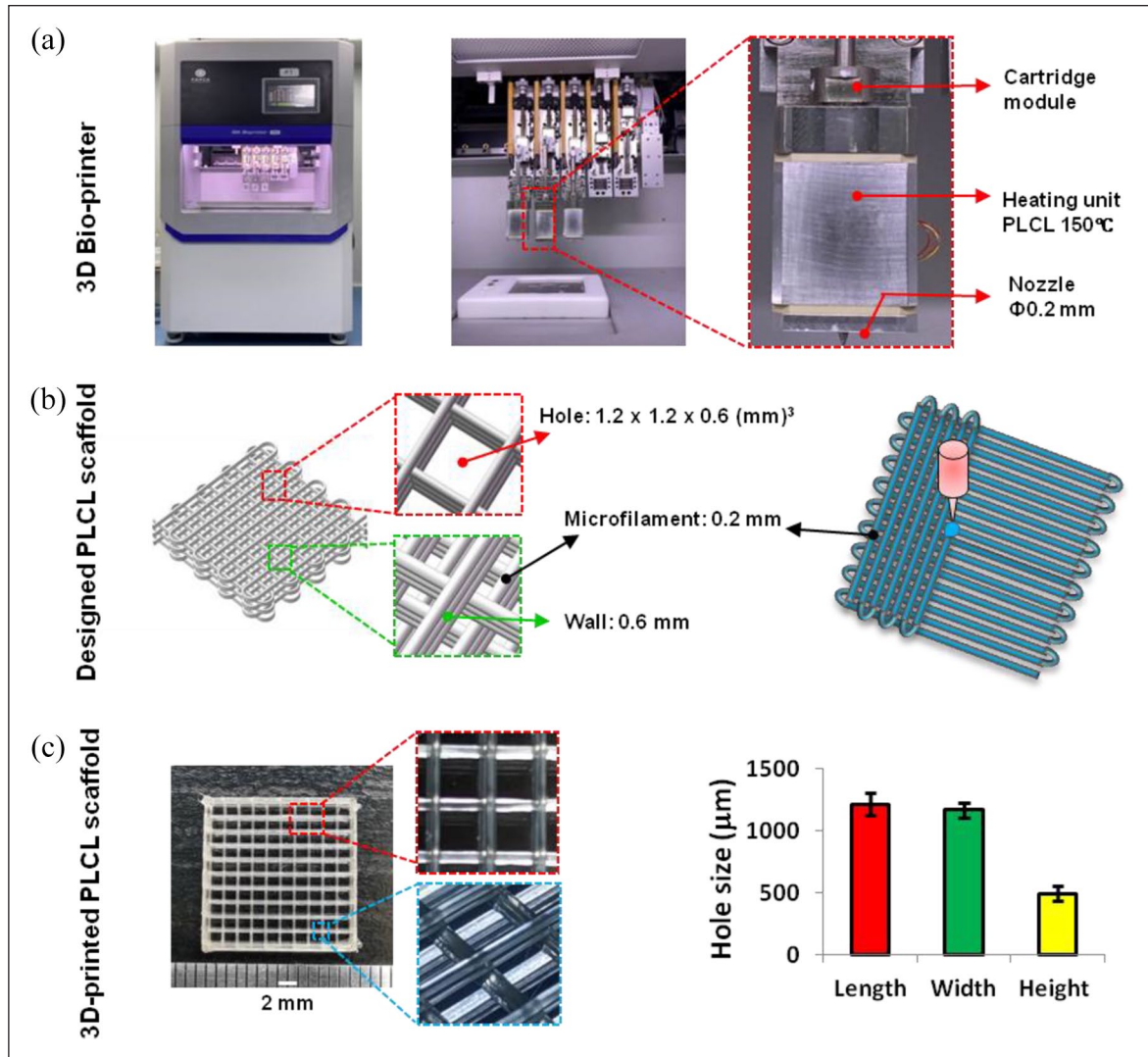
**Figure 1.** Preparation and characterization of tissue engineering skin. (a) Photo images of computer-aided 3D-bioprinter used for 3D-printed PLCL scaffold preparation. (b) Drawn pictures of designed 3D-printed PLCL scaffold showed the structure and printing process. The designed diameter of the microfilament was 0.2 mm (black arrows), each hole was built by three microfilaments (green boxes), and the designed hole size was $1.2 \times 1.2 \times 0.6$ mm$^3$ (red boxes). The scaffold was layer-by-layer printed and the nozzle turned 90° every three layer (left drawn picture). (c) Photo pictures and semi-quantification result showed the morphology of 3D-printed PLCL scaffold which had 100 holes with the average of the length of the hole was $1.21 \pm 0.0898$ mm, the width of the hole was $1.17 \pm 0.0627$ mm, and the height of the hole was $0.49 \pm 0.0583$ mm, respectively. Bar: 2 mm.

clinical and industrial requirements.[25] Our tissue engineering skin was prepared by implanting the MFUS into the 3D-printed PLCL scaffold and sealed with collagen gel. This MFUS-containing 3D-printed PLCL scaffold with collagen gel (PLCL + Col + MFUS) can be used as tissue engineering skin to cover the wound directly. The effect of this novel tissue engineering skin (PLCL + Col + MFUS) on large skin wound healing has been tested by full-thickness skin defect model. To evaluate the survive of the MFUS in the tissue engineering skin, the MFUSs used for the preparation of tissue engineering skin were collected from rat tail skin and implanted into rat dorsal skin wound area due to the MFUS of rat tail

skin differs from rat dorsal skin. The results are reported as the follows.

## Results

### Construction and evaluation of 3D-printed PLCL elastic scaffold

In order to develop tissue engineering skin for enhancing full-thickness wounded skin regeneration, we created PLCL scaffold for carrying MFUS by a 3D bio-printer (Figure 1(a)). The designed diameter of the PLCL microfilament was 0.2 mm printed out by a 0.2 mm nozzle (red
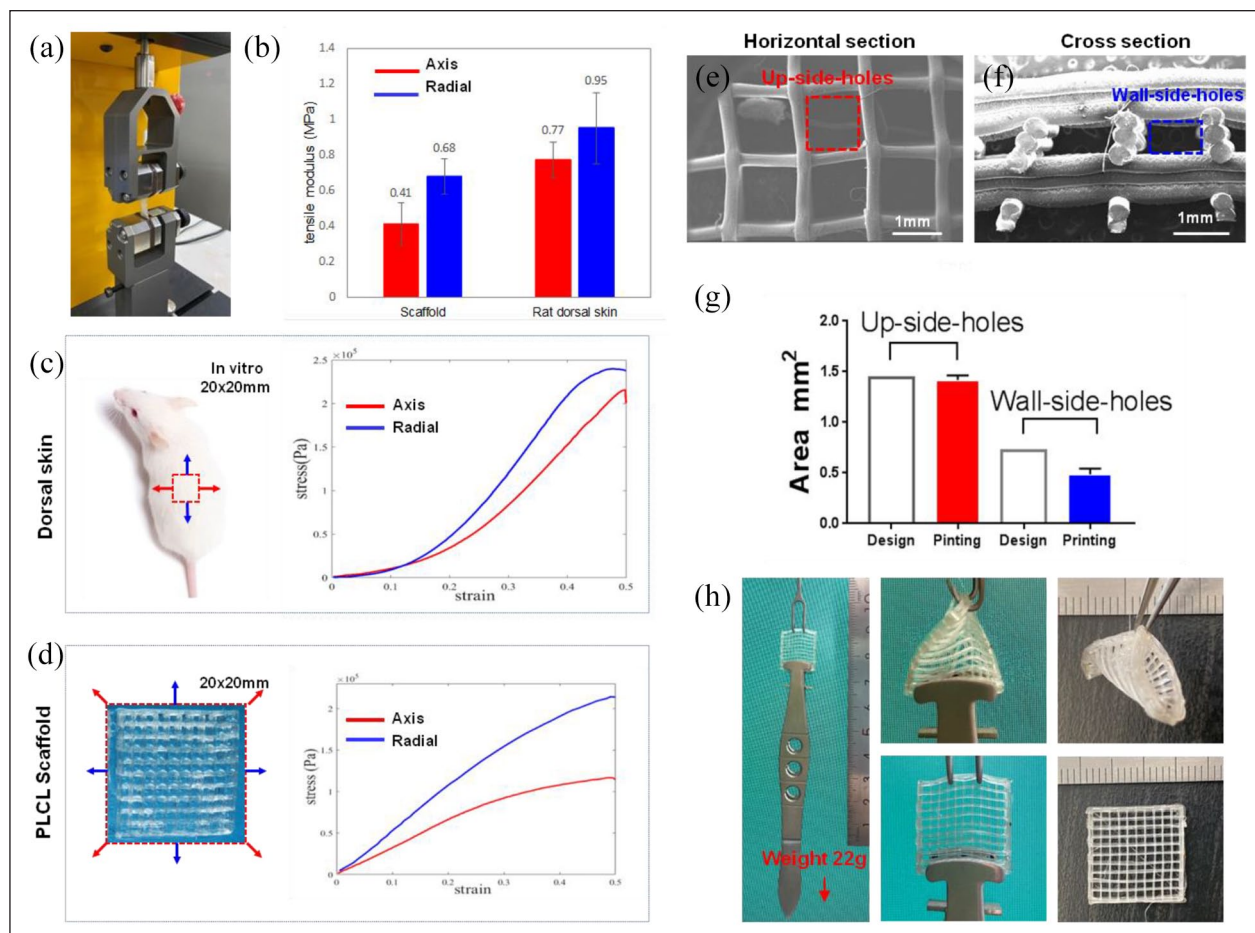
**Figure 2.** Mechanical properties of 3D-printed PLCL scaffold. (a) Photo image showed the equipment (Instron 3400) used for testing the mechanical properties of 3D-printed PLCL scaffold and rat dorsal skin tissues at two positions. (b) The mechanical testing results of 3D-printed PLCL scaffold and rat dorsal skin tissues. (c) Mechanical testing model and results of rat dorsal skin tissues. (d) Mechanical testing model and results of 3D-printed PLCL scaffold. (e) SEM image of the horizontal section of the 3D-printed PLCL scaffold showed the size and structure of up-side-holes. (f) SEM image of the cross-section of the 3D-printed PLCL scaffold showed the size and structure of wall-side holes. (g) Semi-quantification of the holes in the 3D-printed PLCL scaffold compared with the designed hole areas. (h) Elastic testing results demonstrated that there was no any change found in the 3D-printed PLCL scaffold after 180° and 360° stretching test.

box in Figure 1(a)). The scaffold was designed by 100 holes (each hole was 1.2 mm length × 1.2 mm width), and the wall thickness of each hole built by three micro-filaments was 0.6 mm (Figure 1(b)). To ensure the penetration and migration of the cells, and the deposition and distribution of the matrix, the scaffold was printed horizontally at the first three layers, and then the nozzle was turned 90° to print out the other three layers vertically (Figure 1(b)). Finally, the actual thickness of the wall in 3D-printed PLCL scaffold was about $0.49 \pm 0.0583$ mm, the length of the hole was $1.21 \pm 0.0898$ mm, and the width of the hole was $1.17 \pm 0.0527$ mm (Figure 1(c)).

The equipment (Instron 3400) shown in Figure 2(a) was used for testing the mechanical properties of 3D-printed PLCL scaffold with the same models used for rat dorsal and tail skin tissue testing (Figure 2(b)–(d)). The results

indicated that 3D-printed PLCL scaffold was a flexible and elastic scaffold with the similar mechanical properties to rat dorsal skin at all testing positions under 30% strain (Figure 2(b)–(d)). Considering the particularity of the square structure in 3D-printed PLCL scaffold, the central positions on the both sides were chosen for the radial stretching, and the diagonal directions were chosen for the axis stretching (Figure 2(d)). The results showed that the mechanical property of the 3D-printed PLCL scaffold on anti-axis force was weaker than anti-radial stretching (Figure 2(d)) and also lower than that of rat dorsal skin (Figure 2(c)) when they were applied to more than 30% of strain (Figure 2(b)–(d)).

Scanning electron microscopy (SEM) image analysis showed that the 3D-printed PLCL scaffold had well organized lattice structure (Figure 2(e) and (f)). The
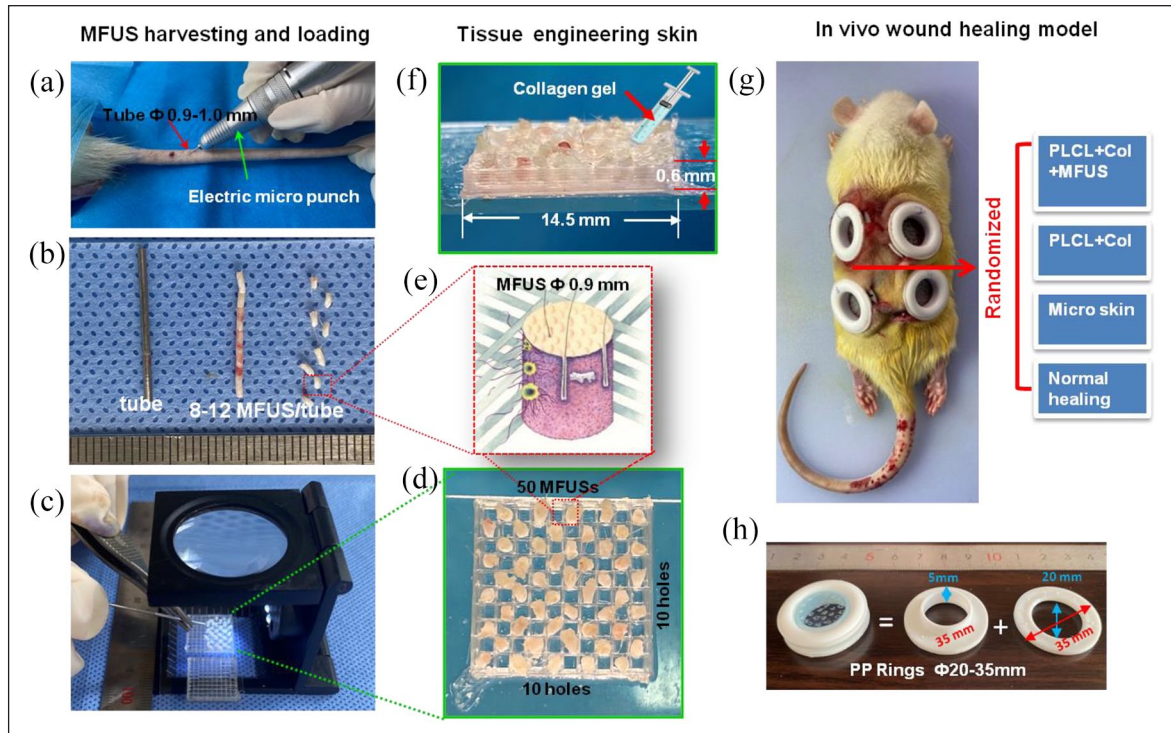
**Figure 3.** In vivo experimental model for large full-thickness skin wound healing. (a) Photo image showed the MFUSs were harvested from rat tail skin using an electric micro puncher. (b) Photo image showed the 8–12 MFUSs harvested and stored in a tube. (c) Photo image showed the MFUS were loaded into the 3D-printed PLCL scaffold using a metal stick under a microscope. (d) Photo image showed total 50 MFUSs have been loaded into 3D-printed PLCL scaffold. (e) A drawn picture showed the structure and the size of the MFUS harvested from rat tail skin tissue (red box in (b)) and loaded into the 3D-printed PLCL scaffold (red box in D). (f) Photo image of tissue engineering skin formed by MFUS-loaded 3D-printed PLCL scaffold with collagen gel. (g) Photo image showed four large full-thickness skin defects have been created in rat dorsal skin and the wound was treated either with tissue engineering skin (PLCL + Col + MFUS), or with scaffold only (PLCL + Col), or with micro skin islands (Micro skin) or without treatment (Normal healing). (h) Photo images showed the structure and the size of the plastic ring used for fixing the wound edge skins.

horizontal section showed that the square holes were separated by the microfilaments (Figure 2(e)), and cross-section showed that each hole was built by three micro-filaments (Figure 2(f)). Semi-quantification showed that the average of the hole areas in the horizontal sections of 3D-printed PLCL scaffold called as up-side-holes (red box in Figure 2(e)) was $1.42 \pm 0.01713\,mm^2$ (designed hole areas: $1.2 \times 1.2 = 1.44\,mm^2$), and the average of the hole areas in the cross-section of the 3D-printed PLCL scaffold called as wall-side-holes (blue box in Figure 2(f)) was $0.4867 \pm 0.0228\,mm^2$ (designed hole areas: $0.6 \times 1.2 = 0.72\,mm^2$) (Figures 1(b) and 2(e)–(g)). Although the wall-side-holes were a little bit of smaller than the designed size due to the scaffold collapsed during the polymer curing (Figure 2(f) and (g)), the up-side-holes still kept the appropriate size for MFUS loading to prepare tissue engineering skin, and the wall-side-holes allowed cell penetration and migration. Further mechanical testing by our designed the device (Figure 2(h)) demonstrated that the 3D-printed PLCL scaffold had very good elastic properties, there was no any changes found

in the scaffold after it was stressed by 22 g with 180° or/and 360° strain (Figure 2(h)).

## Collection of MFUSs and preparation of tissue engineering skin for large full-thickness wounded skin regeneration using an animal model

MFUS as a bioactive source for tissue engineering skin was harvested from autologous rat tail skin using an electric punch with 0.9 mm inner diameter and 1.0 mm outer diameter (Figure 3(a)). The puncher connected a metal tube which can harvest and store 8–12 MFUSs simultaneously in the same direction (Figure 3(b)) and obtain uniform MFUSs in shape (Figure 3(b)). This device can also place the MFUS into the designed position of 3D-printed PLCL scaffold continuously with regard to orientation by using a 0.8 mm diameter of micro poker under microscope (Figure 3(b) and (c)). The tissue engineering skin was prepared by loading one MFUS into one hole of 3D-printed

PLCL scaffold and keeping one hole empty between two MFUSs, total 50 MFUSs were loaded into one piece of 3D-printed PLCL scaffold (Figure 3(d)). To ensure the micro skin island has the minimal functional unit of skin (MFUS), the collected micro skin particle must be full-thickness with one to three hair follicles and some sebaceous glands (Figure 3(e)). The skin surface of the MFUS was loaded as the top side in the 3D-printed PLCL scaffold. Finally, the tissue engineering skin was obtained by the injection of collagen gel into the gaps between the wall of the 3D-printed PLCL scaffold and the MFUS (Figure 3(f)).

Considering the clinical applications, this study collected the MFUS from rat tail skin tissue because rat tail skin tissue has the similar characteristics in the tissue structure and components and the healing process as that of human skin tissue. The effect of tissue engineering skin prepared by MFUS-loaded 3D-printed PLCL scaffold with collagen gel on large full-thickness skin wound healing was investigated by a rat model. Four large full-thickness skin defects at diameter of 30 mm/wound were created in the dorsal skin of rats and treated either with tissue engineering skin (PLCL + Col + MFUS), or with 3D-printed PLCL scaffold and collagen gel (PLCL + Col), or with micro skin island only (Micro skin), or without treatment (Normal healing). Considering the differences among the four wound areas of the dorsal skin, randomly assign was used in selecting each group position (Figure 3(g)). It is well known that the dorsal skin of rats is an elastic tissue which enables it to change its length, volume, or shape in response to a force, followed by recovery toward its original form when the force is removed. To avoid the tissue engineering skin dropping off from the wound area, we designed a concave circular fixation ring to fix each wound area (Figure 3(h)). After the wound was covered with tissue-engineering skin, the wound edge was fixed in the groove of the ring to block the wound edge participating in wound healing and keep the wound moist. The fenestration was removed from the wound area after 1 week to expose the wound.

### Characterization of the MFUS from rat dorsal skin and tail skin

To regenerate the functional full-thickness skin at wound area, we developed a tissue engineering skin by loading micro skin islands into a 3D-printed PLCL scaffold with collagen gel instead of seeding cells to treat large full-thickness skin defect. In order to harvest more micro skin islands in short time, we developed a new electric micro puncher (Figure 3(a)). Our results indicated that this device provided an effective approach for harvesting the micro skin islands quickly with small wound at donor site (Figure 4(a) and (b)). Histological analysis of rat tail skin tissue section at day-21 post-surgery by H&E staining indicated that the wound at donor area has healed with high density

cells (white dash line areas in Figure 4(c)) and some accessory organs including follicles and sebaceous glands were found around the donor wound areas (Figure 4(c)). The wounds at donor areas healed completely at day 60 post-surgery (Figure 4(d)).

Comparing H&E staining results of rat tail skin tissue sections with rat dorsal skin tissue sections, we found that the functional unit is necessary for functional skin regeneration, that means the micro skin island loaded into tissue engineering skin must have a functional unit, otherwise there is no functional skin regeneration if the micro skin island without functional unit. Thus, in this study we proposed a new concept which is called as minimal functional unit of skin (MFUS). H&E staining results indicated that besides the size and distance differences, the MFUS in both skin tissues had the same organs and structures (Figure 4(e)). The MFUS in both skin tissues had a hair follicle in the center and the other six follicles were distributed in the end of hexagonal prism (Figure 4(e)). The healthy normal rat tail skin tissue did not contain subcutaneous muscle layer, the MFUS was centered on three to four rows of transversely arranged 30° oblique caudal hairs, the sebaceous glands were in an elliptical distribution with a diameter of functional unit of 0.85–0.95 mm, and the distance between the center of the unit and the hexagonal end was 0.95–1.05 mm (Figure 4(e) and (f)). The dorsal skin of rats had a subcutaneous muscle layer, the hair was in a single root, the sebaceous glands were underdeveloped, the diameter of the functional unit in rat dorsal skin was 0.35–0.45 mm, and the distance between the center of the MFUS and the hexagonal end was 0.9–1.0 mm, showing a central hexagonal structure (Figure 4(e) and (f)). These results indicated that the MFUS should be harvested from blue circle areas or the end areas of triangles formed by red dash lines of both rat skin tissues, and the size of the MFUS at least should be 0.9 mm (Figure 4(e)).

Our experiment was performed with 0.9 mm diameter circular skin peeling, the pitch of skin was taken 1 mm, each MFUS contained about one to three hairs and their appendages, the residual hair follicles in the donor side grew well (Figure 4(c)), the wounds created by collecting the MFUS underwent scab healing in a time dependent manner (Figure 4(d)), the scab was sloughed off at about 3–4 weeks and completely healed at day-60 post-surgery (Figure 4(d)). Histological analysis by H&E staining showed that these small wounds activated the cells and induced cell migration as evidenced by high cell density found in the wound area (Figure 4(c)). The new formed tissue in the donor site showed normal skin tissue structure as evidenced by the same thickness of each skin layer formed at wound area with some accessory skin organs (Figure 4(c)). These results indicated that MFUS removing by our device did not change the skin structure and functions at donor area and this technique can be used for full-thickness skin defect treatment, and 0.9 mm diameter of
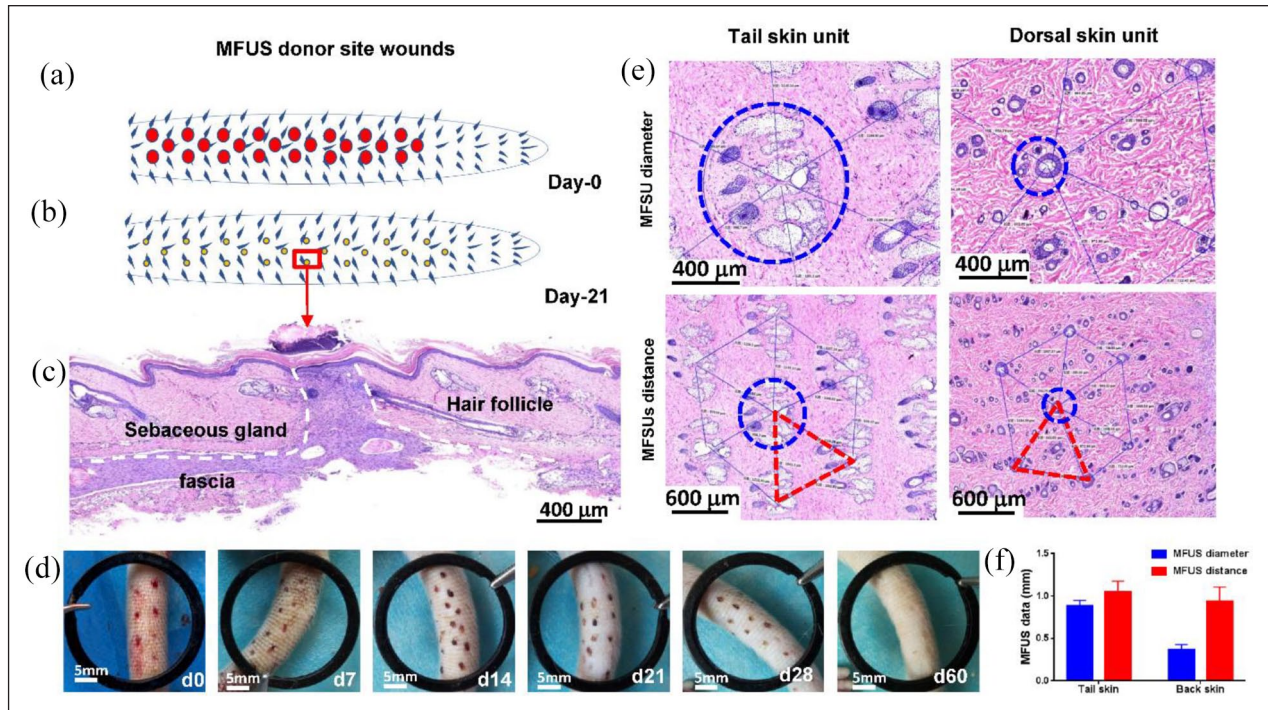
**Figure 4.** Characterization of rat minimal functional unit of skin (MFUS). (a) A drawn picture showed the wounds created in rat tail skin by removing the MFUSs using an electric micro-puncher at day-0. (b) A drawn picture showed the morphology of the wounds at donor areas at day-21 post-surgery. (c) Histological analysis by H&E staining on the rat tail skin tissue section at day-21 post-surgery showed that the wound at the donor area has been healed with high density cells (white dash line areas) and some accessory organs including hair follicles and sebaceous glands. (d) Photo images showed the healing process of the wounds at donor site at different time points. (e) Histology analysis by H&E staining on tissue sections of normal rat tail skin (left two pictures) and rat dorsal skin (right two pictures) indicated that the MFUS of rat tail skin was larger than the MFUS of rat dorsal skin (blue circles and red triangles). (f) Semi-quantification of histological analysis by H&E staining indicated that the average diameter of MFUS (blue dash circle) for rat tail skin was $0.9 \pm 0.15$ mm, for rat dorsal skin MFUS was $0.4 \pm 0.16$ mm, and the average distance between two MFUSs (red dash line) for rat tail skin was about $1.1 \pm 0.21$ mm, and that for rat dorsal skin was $0.92 \pm 0.26$ mm.

each MFUS is the suitable size for wound healing, especially for donor site wound healing.

## Functional skin regeneration enhanced by tissue engineering skin

The effect of tissue engineering skin on large full-thickness wounded skin regeneration was studied by a rat model. Gross view images showed that at d-0 post-treatment, the wounds with the same size were created in all groups (Figure 5(a), (e), (i) and (m)). At day-21 post-surgery, the functional skin with hair follicles and sebaceous glands has been found in the wound area treated with tissue engineering skin (PLCL + Col + MFUS) (Figure 5(b)). The wound treated with 3D-printed scaffold and collagen gel (PLCL + Col) healed faster (Figure 5(f)) than the wounds treated with micro skin (Figure 5(j)) and normal healing wounds (Figure 5(n)), but there was no skin appendages formed in the wound areas treated with PLCL + Col (Figure 5(f)). The results indicated that the 3D-printed PLCL scaffold enhanced wound contraction healing due to the scaffold provided the mechanical attachment points for cell migration.

Without the three-dimensional scaffold support, although the micro skin islands could survive at the wound surface, they grew disorderly and the appearances was uneven because of the mixed positions of the dermis and epidermis in the micro skin islands (Figure 5(i)–(l)). Large unhealed wound areas were still found in normal healing group (Figure 5(n)) with some necrosed tissues and scar tissues (Figure 5(n)). At day-60 post-surgery, the wound treated with functional tissue engineering skin (PLCL + Col + MFUS) healed completely, and gross-inspection showed normal skin covered the wound area (Figure 5(c)). Although the wound treated with MFUS only healed at day-60 post-surgery, some healed skin tissues had no hairs (Figure 5(k)). Some scar tissues were found in the wound areas treated either with PLCL scaffold and collagen gel (Figure 5(g)) or without treatment (Figure 5(o)), but the scaffold treated wound healed much better than the wound without treatment (Figure 5(g) and (o)). The wound healing process in each group was described by drawn pictures, the tissue engineering skin treated wound regenerated the functional skin (Figure 5(d)), the 3D-printed PLCL scaffold and collagen gel treated wound healed faster, but no functional skin regeneration (Figure 5(h)), the micro
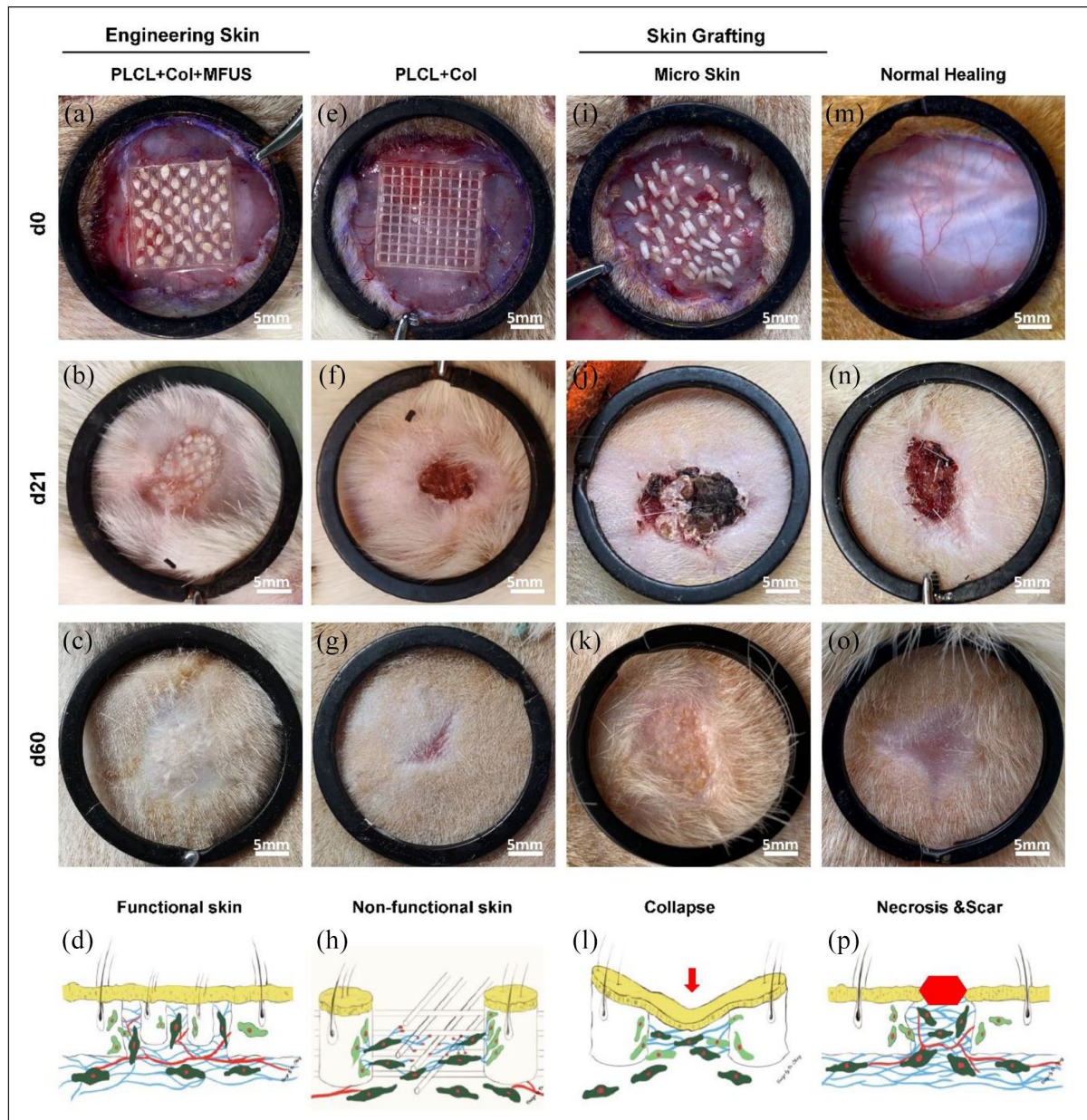
**Figure 5.** Wound healing of full-thickness rat dorsal skin defects with different treatments at different time points. (a–c) Photo images showed the wound treated with tissue engineering skin (PLCL + Col + MFUS) at day-0, day-21, and day-60 post-surgery; (d) A drawn picture shows the functional skin can be regenerated at the wound area treated with tissue engineering skin. (e–g) Photo images showed the wound treated with 3D-printed PLCL scaffold and collagen gel (PLCL + Col) at day-0 and day-21 post-surgery; (h) A drawn picture shows that PLCL + Col treatment can enhance the wound healing, but no functional skin regeneration. (i–k) Photo images showed the wound treated with micro skin islands (Micro skin) at day-0 and day-21 post-surgery; (l) A drawn picture shows that without the scaffold, the micro skin treated wound was collapsed due to some micro skin lost and necrosis. (m–o) Photo images showed the wound without treatment (Normal wound) at day-0 and day-21 post-surgery; (p) A drawn picture shows that without treatment, the wound was healed by scar tissues and left some necrosed tissues.

skin island treated wound healed slower and formed thinner skin (Figure 5(l)), and the wound without treatment healed by scar tissue (Figure 5(p)).

Histological analysis on H&E stained rat dorsal skin tissue sections at day-21 post-surgery showed that the MFUSs have survived in the wound areas treated either with tissue engineering skin (PLCL + Col + MFUS) or with micro skin islands (Micro skin), but the MFUSs grown in the PLCL + Col + MFUS treated wound areas have fused each other (blue box areas in Figure 6(a) and (b)). The MFUSs grew independently in the micro skin treated wound areas (green box in Figure 6(e) and (f)). There was no skin accessory found in the wound areas treated either with 3D-printed PLCL scaffold and collagen
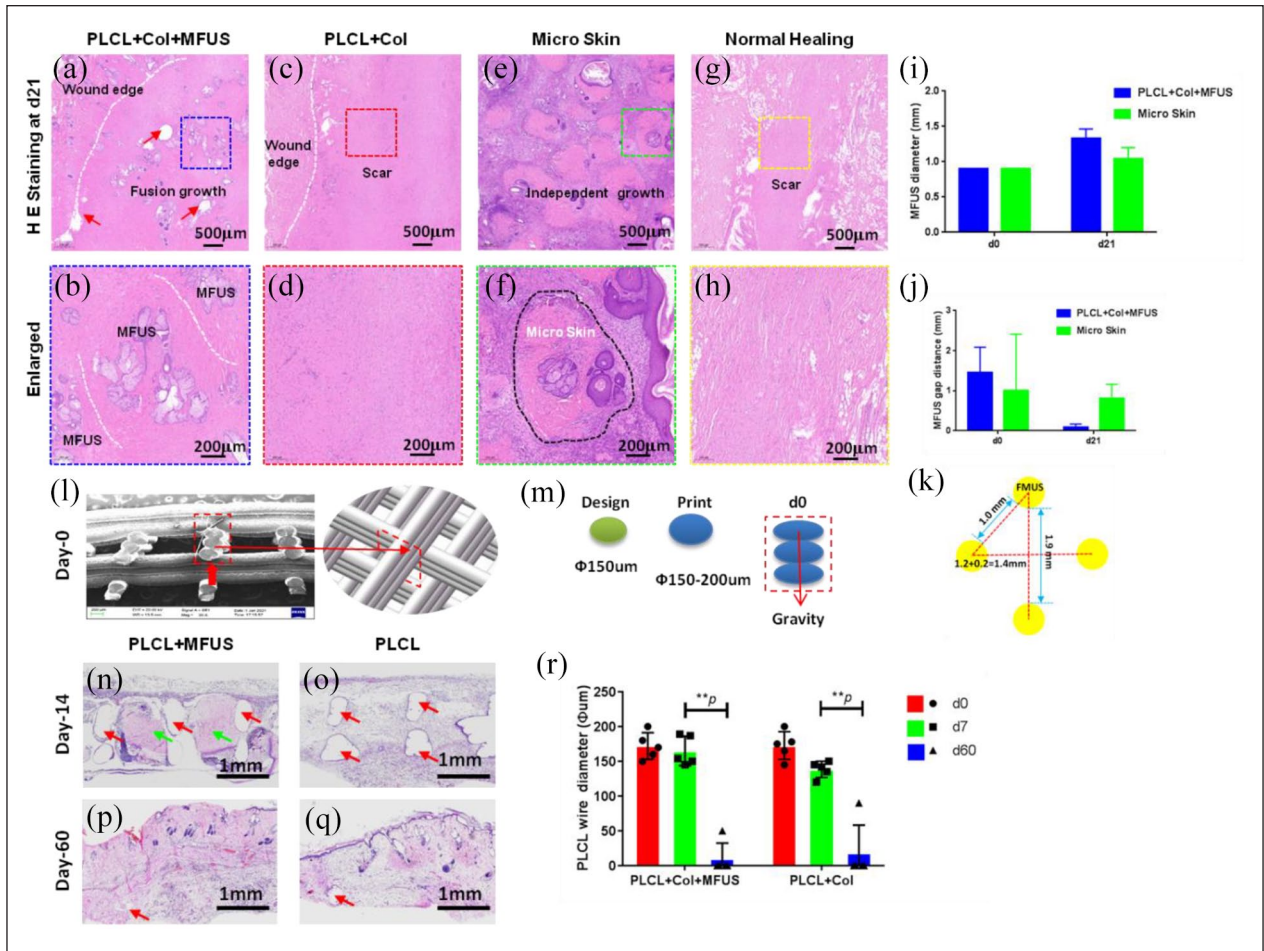
**Figure 6.** H& E staining on the healed rat dorsal skin tissue sections at day-21 post-surgery with four different treatments and the degradation of PLCL scaffold in vivo. (a and b) The wound treated with tissue engineering skin (PLCL + Col + MFUS) healed well and formed functional skin with implanted rat tail MFUS (blue dash box areas). (c and d) The wound treated with 3D-printed PLCL scaffold and collagen gel (PLCL + Col) healed completely, but no functional skin formed in the wound area (red dash box areas). (e and f) The wound treated with micro skin islands healed much better than the normal healing wounds and PLCL + Col treated wounds, but some unhealed areas were still found due to the MFUS lost. The green dash box areas and black dash line areas showed the MFUS survival. (g and h) The wound without treatment (Normal healing) showed many loose collagen fibers in the wound area, indicating the healing is poor and some scar tissues have formed (yellow dash box areas). (i) Semi-quantification of MFUS diameter in the wound areas indicated that the MFUSs have grown up in both treated wound areas, but MFUS grew faster in the wounds treated with tissue engineered skin (PLCL + Col + MFUS) than the wounds treated with micro skin only (micro skin). (j) The gap distance between two MFUSs was much smaller in the wound areas treated with tissue engineered skin (PLCL + Col + MFUS) than that of the wounds treated with micro skin islands (Micro skin). (k) A drawn picture showed the distance between two MFUSs in tissue engineering skin at day-0. White dash lines in (a–h) showed the wound edges, and red arrows in (a) indicated the PLCL scaffold. (l) SEM image of the cross-section of the 3D-printed PLCL scaffold shows the structure and size of the wall of PLCL scaffold at day-0 post-surgery (red box area). (m) Drawn pictures showed the diameter of the designed and printed fiber in 3D-printed PLCL scaffold. (n) H&E staining on the cross section of wounded rat skin treated with tissue engineering skin (PLCL + Col + MFUS) at day-14 post-surgery showed the MFUSs (green arrows) have grown up in the PLCL scaffold. The gap areas (red arrows) showed the scaffold has degraded. (o) H&E staining on the cross section of wounded rat skin treated with 3D-printed scaffold and collagen gel (PLCL + Col) at day-14 post-surgery showed the scaffold has degraded and left the empty gap areas without cells (red arrows). (p) H&E staining on the cross section of wounded rat skin treated with tissue engineering skin (PLCL + Col + MFUS) at day-60 post-surgery showed the PLCL scaffold has degraded completely and the most empty areas have been filled with cells. The empty areas were much smaller compared to the scaffold at day-14 (red arrow). (q) H&E staining on the cross section of wounded rat skin treated with 3D-printed scaffold and collagen gel (PLCL + Col) at day-60 post-surgery showed the scaffold has degraded completely, and the left empty areas were much smaller compared to the scaffold at day-14 (red arrow). (r) Semi-quantification of the H&E staining showed that the wire diameter of the scaffold decreased in vivo in a time dependent manner.

gel (PLCL + Col) (red box areas in Figure 6(c) and (d)) or without treatment (Normal healing) (yellow box areas in Figure 6(g) and (h)).

The micro skin islands were harvested using the same method described for MFUS collection and 50 MFUSs were applied to each wound area of both PLCL + Col + MFUS group and micro skin group. Although the micro skin islands in micro skin group were implanted in the wound area with the same arrangement as tissue engineering skin at day-0 post-surgery, the micro skin islands changed their positions and directions during the animal daily actions due to they don't have scaffold support.

H&E staining results indicated that the healed skin tissues in the wound area treated either with tissue engineered skin (PLCL + Col + MFUS) or with micro skin islands had tail skin structural features (Figure 6(a), (b), (e) and (f)). However, without scaffold supporting, the micro skin islands disorganized in the wound area, and some MFUSs were lost due to the fact that they couldn't adhered tightly to the wound surface (Figure 6(e)). The diameter of the MFUS in the wound areas treated with micro skin islands only expanded from the 0.9 mm at day-0 to 1.04 mm at day-21 (Figure 6(j)), and the diameter of the MFUS in the wound area treated with tissue engineered skin (PLCL + Col + MFUS) has expanded from 0.9 mm at day-0 to 1.33 mm at day-21 (Figure 6(j)).

The gap distance between two MFUSs has been reduced from 1.0–1.9 mm at day-0 to 0.083 mm at day-21 in PLCL + Col + MFUS group, and from 1.0–2.0 mm at day-0 to 0.811 mm at day-21 in PLCL + Col group (Figure 6(j) and (k)). Further study showed that the PLCL scaffold degraded in vivo as evidenced by the wall thickness of the PLCL scaffold determined by H&E staining in the cross sections of rat back skin. The cross-section showed that the thickness of the wall in the scaffold at day-0 was 0.6 mm (Figure 6(l)) which was formed by three micro-fibers with each 0.2 mm diameter (Figure 6(m)). The thickness of the wall in the scaffold in both groups decreased in a time-dependent manner. At day-14 post-surgery, the scaffold degraded and left empty area (red arrows in Figure 6(n) and (o)), and the MFUSs have grown up in the scaffold (green arrows in Figure 6(n) and (o)). At day-60 post-surgery, the scaffold has disappeared completely, and the left empty areas were filled with cells (Figure 6(p) and (q)). Semi-quantification showed less than 10 μm of empty areas found in the healed skin tissues treated either with PCL + Col + MFUS or with PLCL + Col scaffold (Figure 6(r)).

## Functional skin regeneration analyzed by immunostaining

The regenerated skin tissues at wound areas were analyzed by immunostaining on the expression of two vascular cell markers, CD31 and CD34 at day 7 (Figure 7) and two fibroblast cell markers, Engrailed-1 and Neurofibromin at day-60 (Figure 8).

Immunostaining results indicated that the gap areas between MFUS and PLCL scaffold in PLCL + Col + MFUS group (blue box areas in Figure 7(a) and (e)) were filled with new generated blood vessels as evidenced by positively stained cells with CD31 (red fluorescence in Figure 7(a) and (e)) or with CD34 (green fluorescence in Figure 7(a) and (e)) or with both CD31 and CD34 (yellow to orange fluorescence in Figure 7(a) and (e)). Semi-quantification results indicated that the blood vessel density is about 4.22 vessles/$0.002\,mm^2$ in the tissue engineering skin treated wound area (Figure 7(a), (e) and (i)). Although many blood vessels were found in the PLCL + Col treated wound areas (Figure 7(b) and (f)), more than 80% of them were stained positively with CD34 (Figure 7(b) and (f)). The blood vessel numbers in PLCL + Col group were $3.44/0.002\,mm^2$ (Figure 7(i)). Very few blood vessels were positively stained in the gap areas between the micro skin islands (Figure 7(c) and (g)), and the vessels in the micro skin island were strongly stained with CD34 (Figure 7(c) and (g)). The blood vessel density in micro skin treated wound area was $1.78/0.002\,mm^2$ (Figure 7(i)). Normal healing group showed many blood vessels positively stained with CD31 and CD34 in the wound area (Figure 7(d) and (h)) with the density of $7.01/0.002\,mm^2$ (Figure 7(i)).

It is well known that engrailed-1 (EN1) is required for skin scarring.[26] In order to study the mechanism of tissue engineering skin on large full-thickness skin wound healing, we also determined the expression of EN-1 in the wound areas with four different treatments at day-60. Immunostaining results indicated that more than 80% of the cells in the wound areas treated without treatment were positively stained with EN-1 (Figure 8(d), (h) and (i)), however, less than 20% of the cells in the wound areas treated with tissue engineering skin (PLCL + Col + MFUS) were positively stained with EN-1 (Figure 8(a), (e) and (i)). About 38% of the cells in PLCL + Col treated wound area (Figure 8(b), (f) and (i)) and more than 50% of the cells in the micro skin treated wound area (Figure 8(c), (g) and (i)) were positively stained with EN-1.

Neurofibromin (Nf1) is a tumor inhibitor that prevents cell overgrowth by turning off another protein (RAS) which stimulates cell growth and division.[27] It has been reported that when the level of Nf1 increases, the fibroblasts grow slowly, which may reduce the formation of scar tissue. Our immunostaining results indicated that the high levels of Nf1 were found in the wound area treated either with PLCL + Col + MFUS (red fluorescence in Figure 8(a), (e) and (j)) or with micro skin (Figure 8(c), (g) and (j)). A few cells in the wound areas treated either with PLCL + Col (Figure 8(b), (f) and (j)) or without treatment (Figure 8(d), (h) and (j)) were positively stained with Nf1. Semi-quantification of immunostaning on Nf1 indicated that the expression of Nf1 was 76.6% in PLCL + Col + MFUS treated wound, 28% in the PLCL + Col treated wound, 48% in the micro skin treated
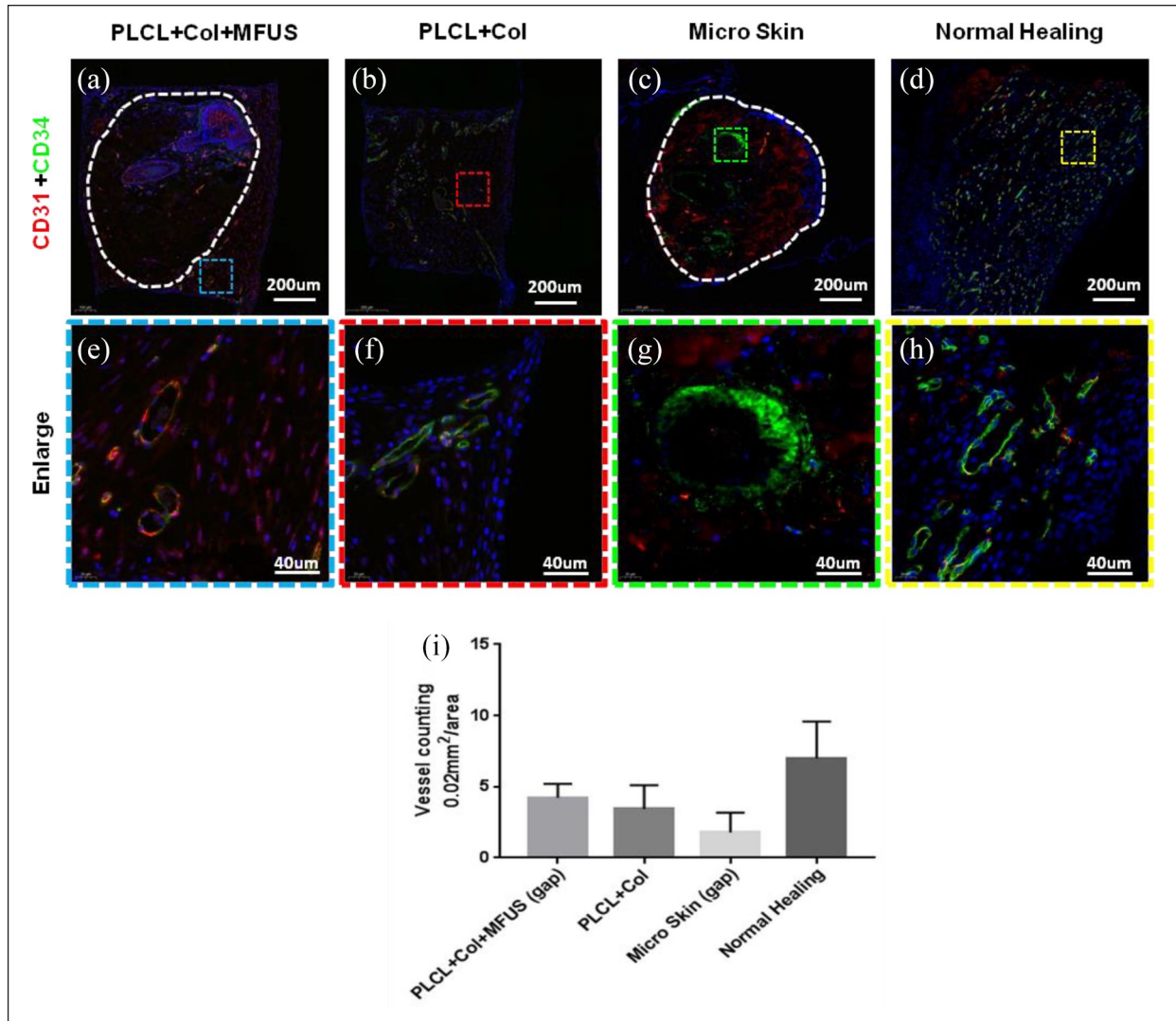
**Figure 7.** Expression of blood vessel markers, CD31 and CD34 on rat dorsal skin tissue sections with four different treatments at day-7 by immunostaining. (a and e) The wound treated with tissue engineering skin (PLCL + Col + MFUS) showed that the vessels not only grew in the MFUS, but also grew in the gap areas (blue box areas) between the MFUSs and the PLCL scaffold. (b and f) The wound treated with PLCL + Col showed many positively stained blood vessels with CD34. (c and g) The wound treated with micro skin islands showed that a few blood vessels in the outside areas of MFUS were positively stained with CD31 and CD34, but some blood vessels in the inside of MFUS were positively stained with CD31 and CD34. (d and h) The wound without treatment (Normal healing) showed that many blood vessels were positively stained with CD31 and CD34. (i) Semi-quantification of the immunostaining results showed that the density of the blood vessels was $4.22/0.002 \, \text{mm}^2$ in PLCL + Col + MFUS treated wound, $3.44/0.002 \, \text{mm}^2$ in PLCL + Col treated wound, $1.78/0.002 \, \text{mm}^2$ in micro skin treated wound, and $7.01/0.002 \, \text{mm}^2$ in normal healing wound.

wound, and less than 20% in the normal healing wound (Figure 8(j)).

## Discussion

In this study, we developed a novel tissue engineering skin by combination of MFUS with 3D-printed PLCL scaffold and collagen gel (PLCL + Col + MFUS) for large full-thickness skin wound healing. Our results demonstrated that this tissue engineering skin has three significances:

The first one is that this tissue engineering skin used 0.9 mm diameter of micro full-thickness skin-island as a minimal functional unit of skin (MFUS) to regenerate full thickness functional skin. Our findings indicated that MFUS is necessary for large full thickness skin regeneration. Without MFUS, there was no functional skin (no follicle and no sebaceous gland) formed in the wound area. The second significance of this tissue engineering skin is that it has a rebar-concrete building-like structure where 3D-printed PLCL elastic microfilament is used as the
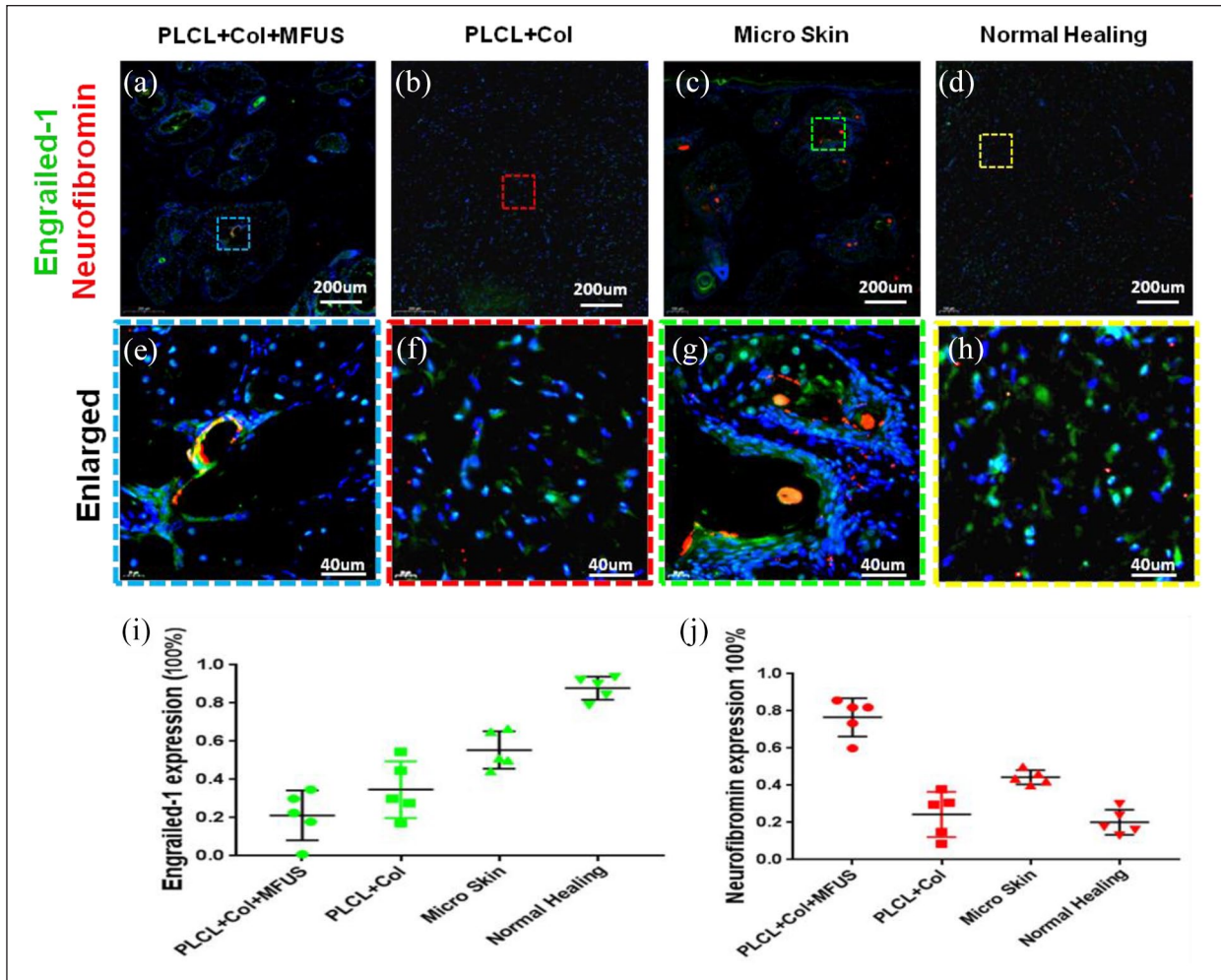
**Figure 8.** Expression of fibroblast markers, engrailied-1 (EN-1) and neurofibromin (Nf1) on rat dorsal skin tissue sections with four different treatment at day-60 post-surgery. (a–h) Immunostaining on engrailied-1 (green fluorescence) and neurofibromin (red fluorescence). (i) Semi-quantification of the engrailied-1 staining results. (j) Semi-quantification of the neurofibromin staining results. (a, e, i and j) The wound treated with tissue engineering skin (PLCL + Col + MFUS) showed that less than 20% of the cells were positively stained with engrailied-1 and more than 76% of the cells were positively stained with neurofibromin in the wound areas. (b, f, i and j) The wound treated with PLCL + Col showed about 38% of the cells were positively stained with engrailied-1, and about 28% of the cells were positively stained with neurofibromin. (c, g, i and j) The wound treated with micro skin islands showed about 50% of the cells were positively stained with engrailied-1 and about 48% of the cells were positively stained with neurofibromin. (d and h–j) The wound without treatment (Normal healing) showed more than 80% of the cells were positively stained with engrailied-1 and less than 20% of the cells were positively stained with neurofibromin.

"rebar skeleton" of the engineering skin, the MFUS is implanted into the 3D-printed PLCL elastic microfilament formed skeleton, and collagen gel used as the "concrete filler" is then added between the microfilament formed walls and MFUS to enhance MFUS survival. The 3D-printed PLCL scaffold not only has very good biocompatibility, but also has suitable pore size designed according to the MFUS size to provide three-dimensional environment for supporting MFUS growth. The third significance of this tissue engineering skin is that collagen gel was used for wrapping MFUS to keep the MFUS in the correct direction and location, and form a simulated extracellular matrix (ECM) microenvironment in which the

scaffold, collagen gel, and local tissue fluid jointly maintained the growth of MFUS.

It is well known that the mechanical properties of PLCL scaffold depend on the ratio of PLA and PCL.[28] This study used 40/60 of PLA/PCL in PLCL copolymer scaffold. The results showed that our 3D-printed PLCL scaffold had the similar mechanical properties as that of rat dorsal skin (Figure 2(b)). Such PLCL copolymer has been used to prepare 3D-printed bio-mimetic wound dressing for skin wound healing.[29,30] It has been reported that the mechanical environment of the wound site is also of fundamental importance for the rate and quality of wound healing.[31] It is known that mechanical stress can influence wound

healing by affecting the behavior of the cells within the dermis.[31] Once the MFUS is removed from the donor site, it will completely lose the support of blood supply and extracellular matrix. When the MFUSs are applied to the wound area, their local mechanical microenvironment has changed greatly. To provide a suitable environment for MFUS growing, we loaded MFUSs into 3D-printed PLCL scaffold with collagen gel together. A number of studies have demonstrated that increased tension promotes the cell proliferation,[32] inhibits cell apoptosis,[33] and activates many signaling pathway that may promote the irregular deposition of ECM.[34] Our results demonstrated that this 3D-printed PLCL scaffold with collagen gel can provide skin mimicking environment for MFUS growing.

In this study, we developed a new electronic puncher for full thickness MFUS collection. Our results indicated that using this device can get MFUS quickly with small trauma at donor site. We found that the defect with 0.9 mm diameter at SD rat tail (donor side) could be recovered by self-regeneration. It has been reported that the meshed skin can be expended to cover wounds larger than the donor site.[35,36] Our results have demonstrated that 0.9 mm diameter MFUS is suitable size for large full-thickness skin wound healing without hurting the donor side tissues.

An important finding of this study is that the minimal functional unit of skin (MFUS) in healthy rat tail and dorsal skin tissues has a equilateral triangle structure which has one MFUS in the center, and the other six MFUSs occupy the each end of hexagonal (Figure 4(e)). This hexagonal structure may be the best optimal angle for keeping skin stress and function. In the future study, we should design/prepare a new 3D-printed scaffold with a hexagonal structure used as a MFUS carrier in tissue engineering skin.

A problem with micro-skin grafting is applying the skin pieces with the dermal side facing the wound surface.[7] To resolve this issue, some researchers have tried to suspend the skin pieces in saline and allowing the skin pieces to "float" to the surface.[37] Although the skin pieces theoretically should float to the top with their epidermal side facing upward, some skin pieces were facing their dermal side upward. Moreover, some skin pieces are lost due to adherence to the bottom or wall of the container during the floatation process.[7] In order to ensure that the MFUS can keep the correct direction and location, we harvested MFUS by an electronic puncher which can keep 8–12 full thickness MFUSs in the same direction for loading. We used 3D-printed PLCL scaffold as MFUS carrier which has suitable pore size for MFUS loading and growing. In the next step, we will continue to study the automatic equipment for loading MFUS combine with the 3D printing process.

The extracellular matrix (ECM) is a key component in the healing tissue. Collagen represents the most abundant interstitial ECM of skin.[38] It has been reported that collagen dressing can recruit several cell types to the wound site, help maintain moist wound environment by absorbing wound exudates, and deactivate excessive matrix metalloproteases.[39] Therefore, collagen type I was selected to fill the gap between the scaffold and the MFUS in this study to form tissue engineering skin. This MFUS-containing 3D-printed PLCL scaffold with collagen gel provided an efficacious approach for large full thickness skin wound treatment.

Neovascularization represents an essential component in wound healing due to its fundamental impact from the very beginning after skin injury until the end of the wound remodeling. In this study, two endothelial cell makers, CD31 and CD34 were found in all wound areas, but the levels of CD31 were much lower in the wound areas treated with tissue engineered skin (PLCL + Col + MFUS) compared to 3D-printed PLCL scaffold and collagen gel (PLCL + Col) treated wounds. Our results indicated that the most of CD31$^+$ and CD34$^+$ cells in the wound area treated with 3D-printed PLCL scaffold and collagen gel (PLCL + Col) were endothelial cells as evidenced by blood vessel-like structure. However, most CD31$^+$ and CD34$^+$ cells in the wound area treated with tissue engineered skin (PLCL + Col + MFUS) were not only endothelial cells, but also some different type cells as evidenced by some positively stained cells without blood vessel-like structure.

Scar formation is more severe when the subcutaneous fascia beneath the dermis is injured upon surgical or traumatic wounding.[40] A recent study has found that injury triggers a swarming-like collective cell migration of fascia fibroblasts that progressively contracts the skin and form scars.[40] To reduce excessive scarring in wound healing, some researchers used polymer meshes as a wound dressing to treat wound.[41] In this study, we added a plastic clip between the 3D-printed PLCL scaffold with/without MFUS and the wound edge skin to block the upper layer skin cell migration. It is well known that skin wounds generally heal by scarring, a fibrotic process mediated by the Engrailed-1 (En1) fibroblast lineage. Scar tissues differ from the normal healthy skin in three ways: (i) They lack hair follicles, sebaceous glands, and other dermal appendages; (ii) They contain dense, parallel extracellular matrix fibers rather than the "basket-weave" pattern of uninjured skin; and (iii) as a result of this altered matrix structure; they lack the flexibility and strength of the normal skin. However, little is known about the cellular and molecular mechanisms blocking a regenerative healing response in postnatal skin, or whether these mechanisms can be bypassed by modulating specific fibroblast lineages. A successful scar therapy would address these three differences by promoting re-growth of dermal appendages, reestablishment of normal matrix ultra-structure, and restoration of mechanical robustness.

Recent studies have shown that Engrailed-1 (EN-1) and Neurofibromin (Nf1) play an important role in wounded

skin healing.[26] When the EN-1 concentration was increased, the skin wound was healed by scar tissue. The basic function of neurofibromin protein is modulation of the RAS protein activity necessary for regulation of cell proliferation and differentiation.[27] It has been reported that neurofibromin is required for skeletal muscle development.[2] Our results showed that low levels of Engrailed-1 and high levels of neurofibromin were expressed in the wound areas treated with PLCL + Col + MFUS. High levels of EN-1 and low levels of neurofibromin were found in the wound area without treatment, indicating the scar tissue formation.

This study provides an efficacious approach for large full thickness skin wound treatment by using a tissue engineering skin consisted of MFUS-containing 3D-printed PLCL scaffold and collagen gel. This new tissue engineering skin can enhance large functional full thickness skin regeneration with minimal scar formation.

## Conclusion

In this study, the effect of tissue engineering skin consisted of MFUS-containing 3D-printed PLCL scaffold with collagen gel on large full-thickness skin regeneration has been investigated. The MFUS was harvested from the rat tail skin and used to treat rat large full thickness dorsal skin defect. The MFUS grown in a mimicking skin microenvironment provided by 3D-printed PLCL scaffold and collagen gel has formed a functional full-thickness skin. This MFUS-containing tissue engineering skin promotes large full thickness skin regeneration by inducing the skin fibroblast migration, enhancing blood vessel, and full skin layers construction. This MFUS-PLCL-collagen tissue engineering skin may be applied in clinics to treat large, deep, full thickness skin wound regeneration.

## Experimental section/methods

### Preparation of PLCL scaffold by 3D-printing technique

The PLCL pellets were obtained commercially (Daigang Biomaterials Inc., Jinan, Shandong, China). The 3D-printed PLCL scaffold was printed using a 3D-bioprinter as shown in Figure 1(a) (SIA 3D-Bioprinter Pro; Shenyang, Liaoning, China). The PLCL pellets were added into the heating box and melted at 150°C. Then, PLCL liquid was squeezed from the nozzle along the *X*- and *Y*-axis according to the designed moving track and model parameters controlled by the computer-aided design software. After one layer was printed, the nozzle was raised to a specific height along the *Z*-axis and the process was repeated for three times, then the nozzle was turned 90° and printed another three layers until the scaffold was printed (right drawn picture in Figure 1(b)). The printing speed was 3 mm/s, and the nozzle diameter was 200 μm. In particular,

the scaffold designed in this article used the [0 0 0 90 90 90]$_n$ trajectory planning path when printing (the same printing path was used for every three layers), which can form micro-holes with 1.8 mm high and 1.2 mm × 1.2 mm square in the up-site-holes for MFUS loading and 0.6 mm × 1.2 mm × 1.2 mm in wall-side-holes to facilitate cell migration (Figure 1(b)).

### Morphology and structure of 3D-printed PLCL scaffold

The morphology and structure of 3D-printed PLCL scaffold were determined by digital optical camera (Nikon D3100, Nikon Corporation) and scanning electron microscopy (SEM; Zeiss, German). For SEM testing, the 3D-printed PLCL scaffold was dried at room temperature overnight and sputter coated with gold and tested by SEM with an accelerating voltage of 20 kV in SE mode. The pore size was determined by Image J software and the average pore size was calculated using six samples.

### Mechanical property of 3D-printed PLCL scaffold

The mechanical property of 3D-printed PLCL scaffold was tested by an electronic universal testing machine as shown in Figure 2(a) and analyzed by integrated testing software (Instron, Norwood, MA, USA). The size of the testing samples was $20 \times 20 \times 2$ mm$^3$ ($n = 8$) as shown in Figure 2(d). The rat dorsal skin tissue samples were also tested using the same protocol ($n = 8$) as shown in Figure 2(c). The elastic properties of the 3D-printed PLCL scaffold were also determined using our developed equipment as shown in Figure 2(h).

### Rat large full-thickness skin wound healing model

Sprague Dawley (SD) rats (300–400 g body weight, male, 5 months old) were used as an animal model to test the effect of tissue engineering skin consisted of MFUS with 3D-printed PLCL scaffold and collagen gel on large full-thickness skin wound healing. The use of all animals for this study has been approved by the IACUC (Institutional Animal Care and Use Committee) of General Hospital of Northern Theater Command.

The surgery was operated under anesthesia by the intraperitoneal injection of ketamine (125 mg/kg body weight) and xylazine (10 mg/kg body weight). The hair was removed from the surgery areas using hair clipper, and the surgery area skin was cleaned with 7.5% of providone-iodine and 70% of alcohol. The MFUS was harvested from the rat tail along the direction of hair follicles using an electric micro-puncher (Figure 3(a)). Each MFUS contained one to three hair follicles was implanted into

3D-printed PLCL scaffold and the 3% collagen gel were filled into the gaps between the MFUS and 3D-printed PLCL scaffold to prepare the tissue engineering skin (PLCL + Col + MFUS).

The collagen type I extracted from bovine Achilles tendon was purchased from Tianjin Shiji Kangtai Biomedical Engineering Co., Ltd. (Tianjin, China), and collagen gel was prepared by dissolving 0.3 g freeze-dried collagen tablet with 10 ml of 1% acetic acid to make a 3% collagen solution. The collagen solution was placed in a refrigerator at 4°C until use.

Four large full-thickness skin wounds (30 mm diameter/wound) were created in the back of each rat. The wound was treated either with tissue engineering skin (PLCL + Col + MFUS), or with 3D-printed scaffold and collagen gel (PLCL + Col), or with traditional micro skin grafting (Micro skin), or without treatment (Normal healing). To avoid the healing differences caused by different skin location, four treatments were randomly distributed in four back wounds. To protect the wounds from the infection and contraction healing, each treated wound was fixed with a double-layer annular plastic clip (inner diameter is 20 mm, outer diameter is 35 mm, side depth is 5 mm) with side grooving and covered with ventilation holes-containing 0.5 mm thickness of polyphenylene sulfide (PPS) film. The wound surface was exposed to air at day-7 post-surgery by removing the annular plastic clip and the PPS film. The rats were treated for 60 days. Three rats were sacrificed at each time point, and the skin regeneration at the wound areas were examined by histochemical staining and immunostaining.

### Histochemical analysis by H&E staining on rat wounded skin tissue sections

The harvested rat skin tissue samples were fixed with 4% paraformaldehyde at room temperature for 5 h, embedded in paraffin, and cut into longitudinal and cross sections with a thickness of 5 μm. To visualize skin tissue structures, the tissue sections were examined with hematoxylin and eosin (H&E) staining according to the standard protocol, and stained skin sections were examined under light microscopy (Nikon eclipse, TE2000-U).

### Degradation testing of PLCL scaffold in vivo by H&E staining on rat wounded skin tissue sections

The harvested rat wounded skin tissue samples were collected at different time points and fixed with 4% paraformaldehyde at room temperature for 5 h, embedded in paraffin, and cross sectioned into 5 μm sections. To visualize skin tissue structures, the tissue sections were examined with hematoxylin and eosin (H&E) staining according to the standard protocol, and stained skin sections were examined under light microscopy (Nikon

eclipse, TE2000-U). The diameter of the micro-fiber in the scaffold was calculated by the SPOT software.

### Immunostaining on rat skin tissue sections

The rat skin tissue samples collected from the wound area were mounted in OCT embedding compound and frozen at −80°C. The tissue block was cut into horizontal and cross sections with 5 μm thickness by a cryostat. The tissue sections were incubated either with mouse anti-CD34 antibody (1:350, Abcam, Cambridge, MA) and rabbit anti-CD31 antibody (1:350, Abcam, Cambridge, MA), or mouse anti-Engrailed-1antibody (1:350, Abcam, Cambridge, MA) and rabbit anti-neurofibromin antibody (1:350, Abcam, Cambridge, MA) overnight at 4°C. In the next morning, the sections were washed three times in PBS for 5 min before being incubated for 2 h at room temperature with FITC-conjugated goat anti-mouse IgG secondary antibody (1:500, ThermoFisher Scientific, Waltham, MA) for CD34 and engrailed-1 testing, and Cy3-conjugated goat anti-rabbit IgG second antibody (1:500, Millipore Sigma, Burlington, MA) for CD31 and neurofibromin testing. Slides were washed with PBS for three times, counterstained with 4′,6-diamidino-2-phenylindole (DAPI; 1 μg/ml, Sigma, St. Louis, MO) nuclear stain, and photographed by a fluorescence microscope (Nikon eclipse, TE2000-U).

### Statistical analysis

Each experiment was performed at least three times, and representative data were reported. Data are expressed as means ± standard deviations (SD). Statistical analyses were performed via student's $t$-test using Excel software and Prism 7. Statistical significance was defined by the value of $p < 0.05$.

### Authors contributions

PC, XFZ, and YHL designed the experiments, performed the image study, histochemical staining and immunostaining, analyzed the data, wrote and revised the manuscript. SJL, HRW, LMZ, SL,YBX, and KG prepared scaffold and performed mechanical testing. QS Performed animal experiments. YHL and XFZ are co-corresponding authors and contributed equally to this study. All authors reviewed and approved the final version of the manuscript.

### Declaration of conflicting interests

The author(s) declared no potential conflicts of interest with respect to the research, authorship, and/or publication of this article.

## ORCID iD

Peng Chang 🆔 https://orcid.org/0000-0001-7926-7725

## References

1. Pereira RF, Barrias CC, Granja PL, et al. Advanced biofabrication strategies for skin regeneration and repair. *Nanomed* 2013; 8(4): 603–621.

2. Brohem CA, da Silva Cardeal LB, Tiago M, et al. Artificial skin in perspective: concepts and applications. *Pigment Cell Melanoma Res* 2011; 24(1): 35–50.

3. Pereira RF and Bártolo PJ. Traditional therapies for skin wound healing. *Adv Wound Care* 2016; 5(5): 208–229.

4. Guo S and Dipietro LA. Factors affecting wound healing. *J Dent Res* 2010; 89(3): 219–229.

5. Groeber F, Holeiter M, Hampel M, et al. Skin tissue engineering: in vivo and in vitro applications. *Adv Drug Deliv Rev* 2011; 63(4–5): 352–366.

6. Chua AW, Khoo YC, Tan BK, et al. Skin tissue engineering advances in severe burns: review and therapeutic applications. *Burns Trauma* 2016; 4: 3.

7. Biswas A, Bharara M, Hurst C, et al. The micrograft concept for wound healing: strategies and applications. *J Diabetes Sci Technol* 2010; 4(4): 808–819.

8. Centanni JM, Straseski JA, Wicks A, et al. StrataGraft skin substitute is well-tolerated and is not acutely immunogenic in patients with traumatic wounds: results from a prospective, randomized, controlled dose escalation trial. *Ann Surg* 2011; 253(4): 672–683.

9. Falanga V and Sabolinski M. A bilayered living skin construct (APLIGRAF®) accelerates complete closure of hard-to-heal venous ulcers. *Wound Repair Regen* 1999; 7(4): 201–207.

10. Oniscu GC and Forsythe JL. An overview of transplantation in culturally diverse regions. *Ann Acad Med Singap* 2009; 38(4): 365–5.

11. Orgill DP, Butler C, Regan JF, et al. Vascularized collagen-glycosaminoglycan matrix provides a dermal substrate and improves take of cultured epithelial autografts. *Plast Reconstr Surg* 1998; 102(2): 423–429.

12. Cheshire PA, Herson MR, Cleland H, et al. Artificial dermal templates: a comparative study of NovoSorb™ biodegradable temporising matrix (BTM) and Integra® dermal regeneration template (DRT). *Burns* 2016; 42(5): 1088–1096.

13. Wood FM, Kolybaba ML and Allen P. The use of cultured epithelial autograft in the treatment of major burn injuries: a critical review of the literature. *Burns* 2006; 32(4): 395–401.

14. Kaur A, Midha S, Giri S, et al. Functional skin grafts: where biomaterials meet stem cells. *Stem Cells Int* 2019; 2019: 1286054.

15. Kadam D. Novel expansion techniques for skin grafts. *Indian J Plast Surg* 2016; 49(1): 5–15.

16. Wood FM, Kolybaba ML and Allen P. The use of cultured epithelial autograft in the treatment of major burn wounds: eleven years of clinical experience. *Burns* 2006; 32(5): 538–544.

17. Murray RZ, West ZE, Cowin AJ, et al. Development and use of biomaterials as wound healing therapies. *Burns Trauma* 2019; 7: 2.

18. Leng L, Ma J, Sun X, et al. Comprehensive proteomic atlas of skin biomatrix scaffolds reveals a supportive microenvironment for epidermal development. *J Tissue Eng* 2020; 11: 2041731420972310.

19. Greenwood JE and Dearman BL. Comparison of a sealed, polymer foam biodegradable temporizing matrix against Integra® dermal regeneration template in a porcine wound model. *J Burn Care Res* 2012; 33(1): 163–173.

20. Gümüşderelioğlu M, Dalkıranoğlu S, Aydın RS, et al. A novel dermal substitute based on biofunctionalized electrospun PCL nanofibrous matrix. *J Biomed Mater Res A* 2011; 98(3): 461–472.

21. Mooney DJ, Breuer C, McNamara K, et al. Fabricating tubular devices from polymers of lactic and glycolic acid for tissue engineering. *Tissue Eng* 1995; 1(2): 107–118.

22. Fonseca MJ, Alsina MA and Reig F. Coating liposomes with collagen (Mr 50,000) increases uptake into liver. *Biochim Biophys Acta* 1996; 1279(2): 259–265.

23. Kim J, Lee KM, Han SH, et al. Development of stabilized dual growth factor-loaded hyaluronate collagen dressing matrix. *J Tissue Eng* 2021; 12: 2041731421999750.

24. Boyce ST and Lalley AL. Tissue engineering of skin and regenerative medicine for wound care. *Burns Trauma* 2018; 6: 4.

25. Weng T, Zhang W, Xia Y, et al. 3D bioprinting for skin tissue engineering: current status and perspectives. *J Tissue Eng* 2021; 12: 20417314211028574.

26. Ye H, Zhang K, Kai D, et al. Polyester elastomers for soft tissue engineering. *Chem Soc Rev* 2018; 47(12): 4545–4580.

27. Chung S, Ingle NP, Montero GA, et al. Bioresorbable elastomeric vascular tissue engineering scaffolds via melt spinning and electrospinning. *Acta Biomater* 2010; 6(6): 1958–1967.

28. Fernández J, Etxeberria A and Sarasua JR. Synthesis, structure and properties of poly(l-lactide-co-ε-caprolactone) statistical copolymers. *J Mech Behav Biomed Mater* 2012; 9: 100–112.

29. Liu W, Feng Z, Ou-Yang W, et al. 3D printing of implantable elastic PLCL copolymer scaffolds. *Soft Matter* 2020; 16(8): 2141–2148.

30. Shafiee A, Cavalcanti AS, Saidy NT, et al. Convergence of 3D printed biomimetic wound dressings and adult stem cell therapy. *Biomaterials* 2021; 268: 120558.

31. Evans ND, Oreffo RO, Healy E, et al. Epithelial mechanobiology, skin wound healing, and the stem cell niche. *J Mech Behav Biomed Mater* 2013; 28: 397–409.

32. Webb K, Hitchcock RW, Smeal RM, et al. Cyclic strain increases fibroblast proliferation, matrix accumulation, and elastic modulus of fibroblast-seeded polyurethane constructs. *J Biomech* 2006; 39(6): 1136–1144.

33. Aarabi S, Bhatt KA, Shi Y, et al. Mechanical load initiates hypertrophic scar formation through decreased cellular apoptosis. *FASEB J* 2007; 21(12): 3250–3261.

34. Hinz B, Mastrangelo D, Iselin CE, et al. Mechanical tension controls granulation tissue contractile activity and myofibroblast differentiation. *Am J Pathol* 2001; 159(3): 1009–1020.

35. Peeters R and Hubens A. The mesh skin graft–true expansion rate. *Burns Incl Therm Inj* 1988; 14(3): 239–240.

36. Oien RF, Håkansson A, Hansen BU, et al. Pinch grafting of chronic leg ulcers in primary care: fourteen years' experience. *Acta Derm Venereol* 2002; 82(4): 275–278.

37. Lin TW. An alternative method of skin grafting: the scalp microdermis graft. *Burns* 1995; 21(5): 374–378.

38. Elgharably H, Roy S, Khanna S, et al. A modified collagen gel enhances healing outcome in a preclinical swine model of excisional wounds. *Wound Repair Regener* 2013; 21(3): 473–481.

39. Brett D. A review of collagen and collagen-based wound dressings. *Wounds* 2008; 20(12): 347–356.

40. Jiang D, Christ S, Correa-Gallegos D, et al. Injury triggers fascia fibroblast collective cell migration to drive scar formation through N-cadherin. *Nat Commun* 2020; 11(1): 5653.

41. Kim HS, Chen J, Wu LP, et al. Prevention of excessive scar formation using nanofibrous meshes made of biodegradable elastomer poly(3-hydroxybutyrate-co-3-hydroxyvalerate). *J Tissue Eng* 2020; 11: 2041731420949332.